6 March 1998

ELSEVIER

Chemical Physics Letters 284 (1998) 387–395

CHEMICAL PHYSICS LETTERS

Near-infrared cavity ringdown spectroscopy of water vapor in an atmospheric flame

J. Xie [1], B.A. Paldus [2], E.H. Wahl [3], J. Martin [4], T.G. Owano [3], C.H. Kruger [3], J.S. Harris [2], R.N. Zare

Department of Chemistry, Stanford University, Stanford, CA 94305-5080, USA

Received 6 October 1997; in final form 17 November 1997

Abstract

We have used cavity ringdown spectroscopy (CRDS) to measure near-infrared overtone transitions of water in atmospheric flames (propane premixed jet and laminar methane-air flat flame burner). The strong signal output with a well-defined laser beam direction and the insensitivity to strong background emission present in hostile environments make CRDS ideal for the study of combustion environments. We have obtained spectra of water vapor from within a flame and extracted a profile of the rotational temperature and concentration of water vapor as a function of distance from the plane burner surface. © 1998 Elsevier Science B.V.

1. Introduction

The chemistry taking place in highly luminous environments, such as arcs, plasmas, and flames, is often hidden by radiant background interference. Moreover, direct probing of such hostile environments is generally difficult owing to the high temperatures and pressures that characterize them. Non-invasive optical methods are commonly used, but are often limited by various drawbacks. For example, emission spectroscopy can only provide information on electronically excited species and is therefore 'blind' to ground-state species [1].

One promising strategy is to use a coherent laser beam as the carrier of information about the ground-state population distribution. This technique has the advantage that the intensity of the incident luminous source falls off with the square of the distance from the source, so that its interference can be significantly suppressed by spatial filtering in which the coherent signal is captured. The success of coherent anti-Stokes Raman spectroscopy (CARS) [2] and degenerate four-wave mixing (DFWM) [3,4] in investigating hostile environments is an example of this advantage. However, the quantitative interpretation of both techniques is often limited by the need to understand in great detail the different contributions to these nonlinear spectroscopies. In addition, both CARS and DFWM depend on the square of the species' single quantum state number density, which

[1] State Key Laboratory of Molecular Reaction Dynamics, Dalian Institute of Chemical Physics CAS, P. O. Box 110, Dalian 116023, P.R. China.

[2] Department of Electrical Engineering, Stanford University, Stanford, CA 94305-4070, USA.

[3] Department of Mechanical Engineering, Stanford University, Stanford, CA 94305, USA.

[4] SL Microtest, Wildenbruchstr. 15, 07745 Jena, Germany.

PII S0009-2614(97)01341-9

precludes an easy extension of these techniques to very low sensitivity limits.

We demonstrate in this letter the use of a linear spectroscopy to examine quantitatively species in an atmospheric-pressure flame in which the signal is carried by a laser beam. Specifically, we report the overtone spectra of water vapor recorded from 810 to 820 nm using cavity ringdown spectroscopy (CRDS). The data are analyzed to yield the rotational temperature of water vapor as a function of distance from the flame burner plane.

CRDS is a sensitive, linear absorption technique first introduced by O'Keefe and Deacon [5], which is based on the measurement of losses in a high-finesse Fabry-Perot cavity. Specifically, by measuring the cavity decay time, one can deduce the total cavity losses which include transmission, absorption, and scattering losses of the cavity mirrors, as well as absorption by species inside the cavity. Hence, the absorption spectrum of a specific species can be calculated from a scan of the cavity losses as a function of wavelength. Absolute measurements of absorption cross-sections (or alternately, concentration if the cross-section is well-known) are obtained by subtracting the losses of an empty cavity from those of a cavity containing the desired sample. Because this technique exploits the rate of decay of light inside the resonator, it is insensitive to intensity fluctuations in the light source.

CRDS has been primarily applied to study molecular transitions of gases in cells with light sources ranging from the ultraviolet (UV) [6,7] to the visible [8–10], to the near-infrared [11,12], and even to the mid-infrared [11,13,14]. CRDS has found utility in the study of laser desorbed, jet-cooled organic clusters [15], silicide and metal cluster [16] beams. CRDS has also been used to detect radicals in hostile environments, such as OH in a Bunsen burner [7], HCO in a low pressure flame [17], C_6H in a hollow cathode discharge [18], or CH_3 radicals in a hot-filament reactor [19].

In the present work, we have exploited the sensitivity and versatility of CRDS to study the ground-state molecular species of water vapor in atmospheric-pressure flames. We have investigated the overtone transitions of the O-H vibrations between 810 and 820 nm, with the aim of demonstrating that CRDS can detect weak transitions of reaction products (e.g. combustion products) in hostile environments. The overtone transitions are used because high reflectivity mirrors, as well as high sensitivity and low-noise detectors are not readily available. Furthermore, we have used an OPO laser source in the visible to avoid the problem of long fluorescence tails associated with Ti:sapphire lasers, which makes the latter more difficult to use in CRDS. We also show that this technique remains relatively insensitive to backgrounds radiating over the entire detector responsivity range, as well as to media presenting nonuniformly dense optical paths along the ring-down resonator principal axis.

2. Apparatus and experimental method

A Nd:YAG laser-pumped optical parametric oscillator (OPO) is used to generate nearly Fourier-transform-limited Gaussian light pulses. The pulses are 4 ns in duration and run at a 10 Hz repetition rate. The laser (Continuum Mirage 3000) has an upper linewidth limit of 500 MHz (0.017 cm^{-1}). Infrared radiation is generated by the OPO as follows (cf. Fig. 1a): the master oscillator (MO) KTP crystal is pumped with frequency-doubled, single-mode 532 nm light from a single-mode-seeded Nd:YAG pulsed laser; the MO resonator consists of two mirrors and a grating in a Littrow configuration, which produces single-mode operation; the first order grating deflection is resonantly enhanced in the resonator, while the zeroth order grating deflection provides the MO near-infrared output. This MO output serves as the seed radiation for the optical parametric amplifier stages that mix it with 532 nm and subsequently 1064 nm radiation in order to produce a signal (1.45 μm to 2.12 μm) and an idler (2.12 μm to 4.0 μm). In this experiment, the output from the parametric OPA 1, which is tunable from 710 nm to 850 nm and produces 15 mJ of energy, is used (cf. Fig. 1a).

The MO output is directed onto a ringdown cavity (RDC), along with a collinear HeNe alignment laser (cf. Fig. 1b). The RDC is a linear Fabry-Perot resonator, consisting of two concave mirrors (Newport:10CV00.SR.40F), each having a 99.98% reflectivity and a 1 m radius of curvature. The cavity length is chosen according to Meijer [7], such that a quasi-continuum mode-structure is obtained, allowing high resolution scans to be performed without

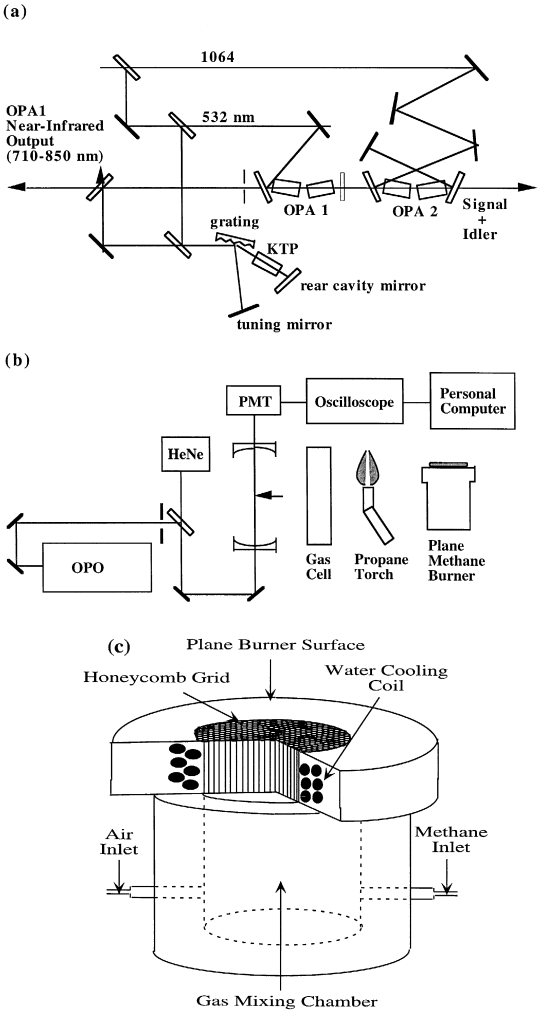

Fig. 1. (a) Generation of near-infrared light in the master oscillator stage of an optical parametric oscillator; (b) experimental setup used to measure water vapor in a gas cell, in a propane torch flame and in a plane methane burner flame; (c) schematic of Meker type burner.

loss of spectral information. Output radiation from the RDC is detected using a near-infrared photomultiplier tube (PMT) with a responsivity from 160 nm to 930 nm (Hamamatsu: R943-02) peaking between 300 nm and 850 nm. The signal is digitized and averaged on an oscilloscope (HP: 54510A, 1GSa/s with 20 single-shot averaging). The logarithm of the ringdown decay is analyzed on a personal computer using a linear least squares fit.

For measurements of water vapor in a closed environment, the two mirrors are mounted as windows (41.5 cm separation) on vacuum cell flanges, thereby sealing the ends. Flexible bellows fixed in gimbal mounts (MDC: FGC-275-M) allow adjustment of the mirrors with micrometer screws. The cell is evacuated with a rotary pump to a residual pressure of 5 mTorr before being filled to a specific pressure with water vapor. For measurements of water vapor generated in a propane torch flame, the central segment of the vacuum cell is removed and replaced with a mount holding the torch, such that the center of the flame is positioned at the height of the RDC axis. Each half segment of the vacuum cell is tapered down from a 1.5'' flange to a 5 mm aperture stainless steel tube, in order to reduce mirror degradation caused by exposure to the flame, and to limit the presence of atmospheric water vapor in the ringdown path. A dry nitrogen gas purge is flowed from the mirrors to the flame to minimize further mirror contamination by water vapor, room dust, soot, and heating by the torch. This purge also eliminates absorption losses caused by water vapor in the ambient atmosphere. The nitrogen flow velocity was adjusted to minimize the shear layer mixing and maintain homogeneity of the flat flame. For measurements of water vapor produced by a plane methane flame, the methane burner was placed at the center of the RDC. Its position relative to the RDC axis is controlled with a variable height mount.

In all combustion experiments, appropriate evacuation of the product gases was achieved using an overhanging duct. The propane flame is generated by igniting flowing propane from a soldering torch (BenzOmatic Propane Fuel Cylinder) and adjusting the propane flow rate until a controllable burn is achieved. No air flow, other than that occurring in the ambient environment is provided to the flame. The 5 cm tall, 1 cm diameter propane flame has a teardrop shape and shows the three typical flame temperature regions: a light blue, low-temperature region near the torch nozzle, a bright yellow, high-temperature region at the flame tip, and a moderate-temperature (ca. 2000 K), blue region elsewhere. Flame height is adjusted until a known region intersected the CRD axis (i.e., the HeNe alignment beam).

The plane flame is generated in a 7 cm diameter water-cooled Meker type [20] burner, shown in Fig. 1c. Both methane and air were supplied at room temperature (293 K) and monitored with calibrated

flow meters (Mathieson). Industrial grade (> 99.9% purity) methane and (> 99% purity) air are mixed to achieve the desired stoichiometry of $\phi = 1.1$, where

$$\phi = \frac{(\text{fuel flow rate})/(\text{air flow rate})}{(\text{fuel flow rate})/(\text{air flow rate})_{\text{stoichiometric}}} \quad (1)$$

i. e., $\phi > 1$ is a fuel rich flame. In these studies, optimal flame stability was obtained with 1.289 slpm methane and 11.15 slpm air flow rates (inlet cold flow velocity of 5.4 cm/s), and resulted in a flat flame luminous zone with minimal curvature.

3. Results and discussion

Using an optical parametric oscillator light source for conventional pulsed CRDS, shown in Fig. 1, we were able to obtain spectra of water vapor in ambient air, at the center of a propane torch flame, and at various heights of a flat flame methane-air burner, as shown in Fig. 2. All measurements were carried out at atmospheric pressure, so that all lines are pressure broadened to at least several GHz. After background subtraction, no baseline adjustments have been made.

Overall, our spectra compare favorably in absolute frequency, linestrength, and linewidth, to those generated using the HITRAN96 and HITEMP databases [21]. HITRAN is an acronym for high resolution transmission molecular absorption database, while HITEMP is the high temperature equivalent of HITRAN for temperatures ranging from 1000°C to 1500°C (http://www.hitran.com). Using these databases in addition to the extensive tabulation of near-infrared water lines in Toth [22] and Flaud [23], we were able to assign all lines at 300 K and most (ca. 98/at high temperatures (> 1000 K) in the flames. Over our scanning range, we primarily observed rotational branches from the $2\nu_1 + \nu_2 + \nu_3$ vibrational band, in particular the P_{01}, Q_{01}, and R_{01} branches, but we also recorded rotational lines from the $\nu_1 + \nu_2 + 2\nu_3$ and $3\nu_1 + \nu_2$ vibrational bands. Spectral assignments corresponding to lines shown in Fig. 2 and Fig. 3 are listed in Table 1. The notation used to identify a specific rotation line is (J, K_a, K_c), where K_a is the value of $|K|$ for the

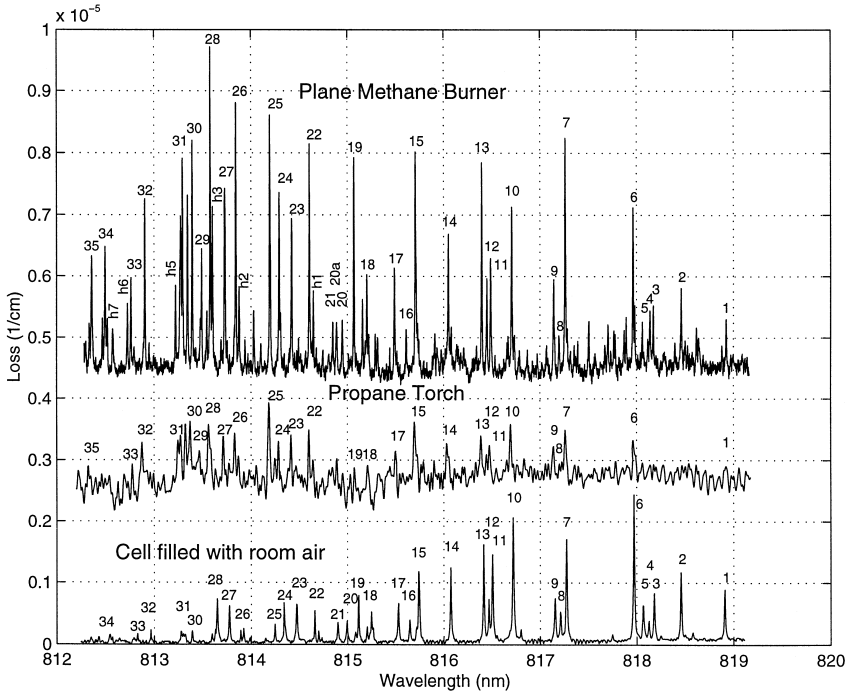

Fig. 2. Spectra of water vapor in (a) a vacuum cell at 20 Torr and 300 K, (b) a propane torch flame at atmospheric pressure and 2000 K, and (c) a plane methane burner flame at atmospheric pressure and 5000 K.

limiting prolate symmetric top with which the rotation level correlates, while K_c is the value of $|K|$ in the oblate rotor limit. For additional information on these transitions (e.g. line intensity, lower state energy, pressure-broadening coefficients, etc.), the reader is referred to the HITRAN96 and HITEMP databases, as well as tabulations by Toth [22] and Flaud [23].

The emergence of 'hot bands' between 813 and 815 nm in the flame spectra is illustrated in Fig. 2. A more detailed comparison of spectra taken at various heights above the flat flame methane-air burner is presented in Fig. 3. Changes in population among rotational states within the $2\nu_1 + \nu_2 + \nu_3$ vibrational band occur as detection moves farther away from the burner surface and the water vapor generated by combustion cools. At higher temperatures, rotational states with higher J become populated at the expense of lower J states, as expected from Boltzmann's distribution of rotation states $n(J,K_a,K_c)$ of water vapor [24]:

$$n(J,K_a,K_c,\nu_i) = n_{\text{tot}}\frac{g(J,K_a,K_c)}{Q(T)}\exp\left(-\frac{E(J,K_a,K_c,\nu_i)}{kT}\right), \quad (2)$$

where n_{tot} is the total concentration, ν_i is the vibrational band state, (J,K_a,K_c) define the rotational state, $E(J,K_a,K_c,\nu_i)$ is the energy level of the state, $Q(T)$ is the internal partition function [25], $g(J,K_a,K_c)$ is the degeneracy function, k is the Boltzmann constant, and T is the temperature. It is possible to relate the population of a rotational state to the integrated absorption measured via the line intensity, I_s, [24]:

$$I_s = \frac{\pi e^2}{m_e c^2} n(J,K_a,K_c,\nu_i) f(J,K_a,K_c), \quad (3)$$

and to obtain a direct measure of the transition strength which is entirely independent of lineshape. Hence, by measuring the integrated absorption of various rotational branches within the $2\nu_1 + \nu_2 + \nu_3$ transition, namely the Q_{01} and R_{01} branches ($5 \le J \le 20$, $0 \le K_a \le 3$), and by fitting for the slope of $\ln(I_s/g(J,K_a,K_c))$ versus $E(J,K_a,K_c)$, the rotational temperature was obtained. In this calculation, the degeneracy factors $g(J,K_a,K_c)$ were calculated from HITEMP line intensities by using the lower state energy, the transition probability, and air-broadened linewidths provided HITEMP, as well as an empirical temperature-dependent partitition function provided by Pierrot [25]. An iterative procedure that minimizes the least squares error of the fit and accounts for the temperature dependence of both line intensity and partition function, was used to determine the slope. The final temperature at any given distance above the burner is an average over at least five temperatures obtained from different subbranches in which K_a is held constant and J and K_c are varied. Each subbranch contains at least 8 lines spanning at least 1.5 kT in lower state energy. The inset in Fig. 4a shows a typical straight line fit for a rotational branch; the quality of the fit demonstrates that the assumption of local thermal equilibrium remains valid.

A plot of temperature versus distance for the flat flame methane-air burner is shown in Fig. 4a, along with experimental results for $\phi = 0.9$ [26], theoretical results for $\phi = 1.0$ [27], and measured temperatures in the constant region for $\phi = 1.1$ [26]. From Fig. 4, it is clear that our measured temperature profile lies within the temperature interval for $\phi = 1.1$ given in Cattolica [26] for an identical methane-air burner, and is within 200 K of the adiabatic flame temperature. Furthermore, our temperature profile

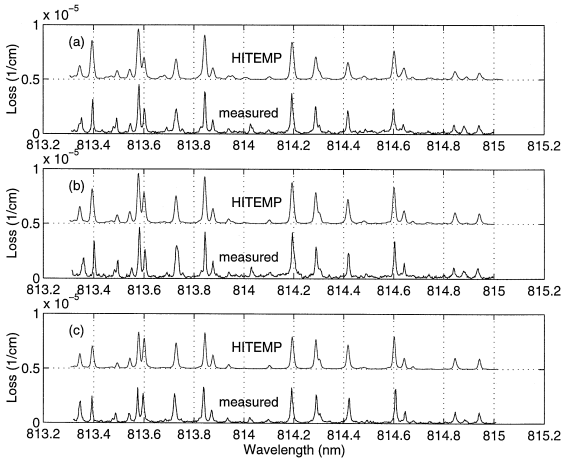

Fig. 3. Spectra of water vapor generated by a plane methane burner at (a) 0.12 cm, (b) 3.1 cm, and (c) 10.0 cm above the burner grid.

Table 1
Line assignments for water vapor transitions from (J,K_a,K_c) to (J',K_a',K_c'). Doublets are listed under only one reference number with primes indicating the weaker line(s)

Line	Wavenumber (cm^{-1})	Vibrational band	(J',K_a',K_c') ← (J,K_a,K_c)
1	12212.070	211	(303) ← (202)
2	12218.829	211	(322) ← (221)
3	12223.804	211	(414) ← (313)
4	12223.848	211	(321) ← (220)
5	12224.682	211	(312) ← (211)
6	12226.101	211	(484) ← (303)
7	12236.560	211	(515) ← (414)
8	12237.466	211	(423) ← (322)
9	12238.312	211	(505) ← (404)
10	12244.719	211	(413) ← (312)
10'	12244.787	211	(431) ← (330)
11	12248.020	211	(422) ← (321)
12	12248.579	211	(616) ← (575)
13	12249.390	211	(686) ← (505)
14	12254.518	211	(524) ← (423)
15	12259.602	211	(717) ← (616)
15'	12259.477	211	(707) ← (606)
15''	12259.95	310	(423) ← (312)
16	12260.995	211	(514) ← (413)
17	12262.813	211	(533) ← (432)
18	12267.038	211	(625) ← (524)
18'	12267.028	211	(542) ← (441)
18''	12266.7483	211	(532) ← (431)
18'''	12267.6810	211	(818) ← (717)
19	12268.998	211	(808) ← (707)
19'	12269.487	310	(524) ← (413)
20	12270.814	211	(523) ← (422)
20a	12271.565		(12 3 9) ← (11 3 8)
21	12272.276	310	(625) ← (514)
22	12275.935	211	(919) ← (818)
23	12278.720	211	(615) ← (514)
23'	12277.967	211	(744) ← (725)
24	12280.663	211	(726) ← (625)
24'	12280.438	211	(634) ← (533)
25	12282.104	211	(10 0 10) ← (909)
26	12286.893	211	(541) ← (642)
26'	12287.379	211	(11 1 11) ← (10 1 10)
27	12289.131	211	(633) ← (532)
27'	12289.067	211	(716) ← (615)
28	12291.046	211	(624) ← (523)
29	12291.380	211	(12 0 12) ← (11 0 11)
29'	12291.908	211	(827) ← (726)
30	12294.907	211	(817) ← (716)

Table 1 (continued)

Line	Wavenumber (cm^{-1})	Vibrational band	(J',K_a',K_c') ← (J,K_a,K_c)
31	12296.058	211	(735) ← (634)
32	12301.523	211	(928) ← (827)
33	12303.651	211	(744) ← (643)
34	12307.601	211	(10 1 9) ← (918)
34'	12307.989	211	(725) ← (624)
35	12294.165	211	(13 1 13) ← (12 1 12)
h1	12275.331	211	(909) ← (808)
h2	12285.707	310	(21 1 21) ← (20 1 20)
h3	12291.052	211	(624) ← (523)
h4	12294.906	211	(817) ← (716)
h5	12296.342	211	(15 1 15) ← (14 1 14)
h6	12304.194	211	(918) ← (817)
h7	12306.450	211	(743) ← (642)

follows closely, although at slightly higher levels than expected for a fuel-rich stoichiometry, the temperature profile in Cattolica [26].

In order to extract the mole fraction of water vapor produced in the flame as a function of distance, recourse was made to the HITEMP database. Once knowledge of the temperature was obtained for a given point, it was possible to calculate the integrated line intensities from HITEMP for specific rotational lines [5]. The mole fraction, ψ, is then simply given by the ideal gas law for a fixed temperature and volume:

$$\psi_{H_2O} = \frac{n_{H_2O}}{n_{tot}} = \frac{p_{H_2O}}{p_{tot}} = p_{H_2O}(\text{atm}) \qquad (4)$$

for a 1 atm flame, where n is the number of moles, and p is the pressure. A plot of mole fraction of water vapor versus distance from the burner surface is given in Fig. 4b, along with the adiabatic peak mole fraction for $\phi = 1.1$, and a theoretically predicted distribution for $\phi = 1.0$ from Tsatsaronis [27]. The mole fractions plotted are an average over six rotational lines with $4 \le J \le 7$, $1 \le K_a \le 3$, and $2 \le K_c \le 6$ in the $2\nu_1 + \nu_2 + \nu_3$ vibrational band.

The measured data were interpolated, and this interpolation lies in between the theoretically predicted profile and the adiabatic limit, as would be expected for a fuel-rich ($\phi > 1.0$) stoichiometry.

[5] These integrated intensities can be converted from the standard HITEMP units of $cm^{-1}/(molecule/cm^2)$ to cm^{-2}/atm, by applying a factor of 2.48×10^{19} (at 273 K, and scaled according to the species temperature), so that partial pressures of water vapor can be directly calculated from the measured spectra.

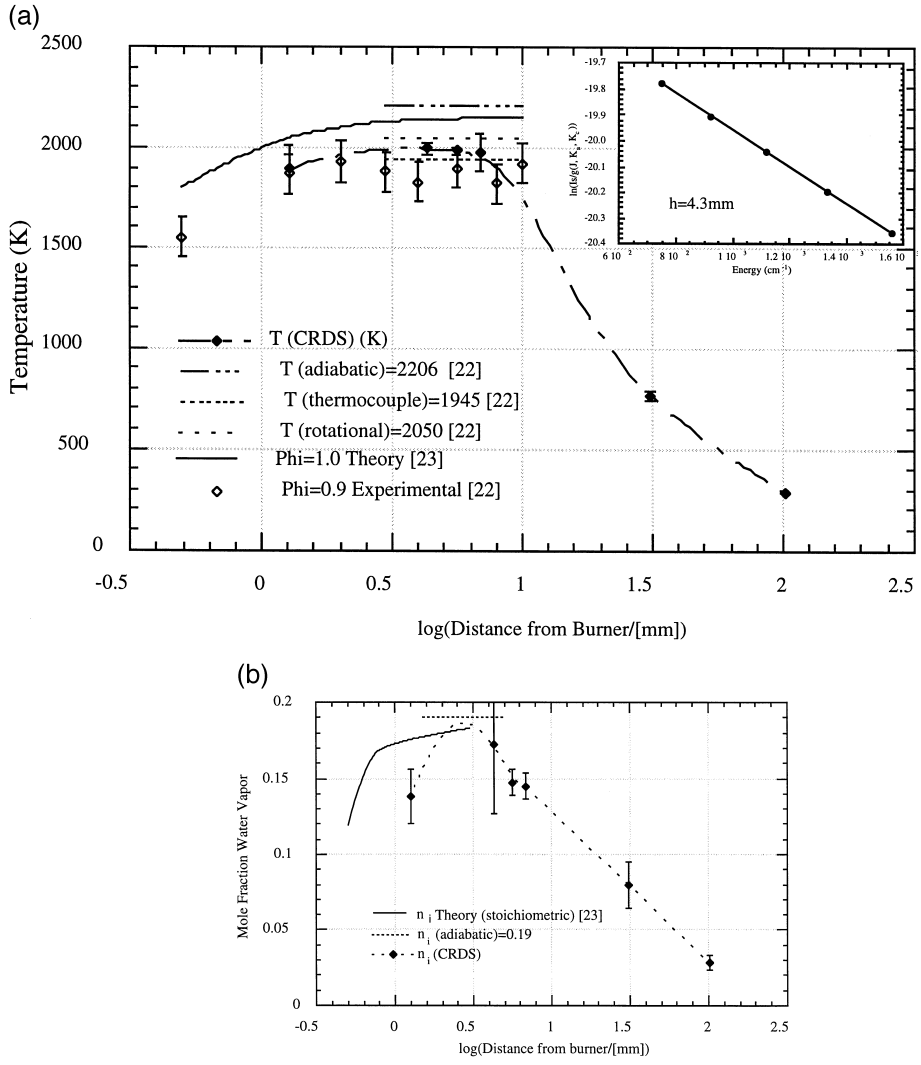

Fig. 4. Water vapor (a) temperature and (b) mole fraction as a function of distance from a plane methane burner grid.

Because the majority of our data points lie outside the theoretical region of [27], their lower mole fraction can be attributed to the rapid diffusion of water vapor above the burner surface, which is amplified with distance, and directly corresponds to the lower temperatures observed. Moreover, the data points within the theoretically predicted region possess fairly substantial error bars, indicating that significant measurement uncertainty exists. Finally, the overall lower mole fractions measured could be caused by perturbation of the burner stoichiometry and gas flow by the nitrogen purge (used to protect the high reflectors). Although the purge was not observed to cause flame instability, it nonetheless increases the total nitrogen present in the flame, and could therefore cool the flame.

A detection limit of 8×10^{-9} cm^{-1} for 99.99% mirrors was calculated from the RMS baseline noise in an evacuated cell, divided by the quantity $L/(1-R)$, where L is the cavity path length and R is the mirror reflectivity. In the spectra of Fig. 2, however, the baseline RMS noise is increased from that of the evacuated cell: by a factor of 1.6 for measurements of ambient air in the cell; by a factor of 4.5 for the

flat flame methane-air burner; and, by a factor of 25.2 for the propane torch. In addition, the flame spectra show irregular undulations in the baselines, even after background subtraction, which are greatest in the propane torch spectrum. The increase in baseline noise from an evacuated cell to one filled with ambient air is consistent with our previous results [12], and has been attributed to the presence of dust and other airborne particles or droplets in the environment. The change in baseline noise from the presence of flames is much larger, with the largest increase observed for an uncontrolled burn in the narrow propane jet. Because care was taken in the combustion experiments to prevent contamination of the mirrors by using a nitrogen purge, the increase in the flame baseline noise seems to originate in the flame media itself. There are several possible causes for the significant increase in flame baseline noise which result in 'fast' fluctuations and 'slow' baseline drift.

Rapid baseline fluctuations may be caused by both the nonuniformity and the luminosity of the flame media. The laser beam can be scattered by combustion products such as soot, or be rerouted from its linear propagation by local variations in the refractive index of the flame. Because it is impossible to distinguish between these and simple absorptive losses in the ringdown cavity, and because these losses occur randomly over the light path (which is thousands of roundtrips of the cavity), they will contribute noise to the baseline. Furthermore, the luminous output of the flame will also contribute to the noise because stray photons will pass through the output CRD mirror (which is only highly reflecting for 30 nm in the infrared, but will pass visible and UV light) to the PMT, and produce noise on the ringdown decay waveform. This noise translates into an increased fitting error and consequently baseline noise. A red filter was used in the experiment to reduce this stray output radiation.

Slow fluctuations of the baseline may be produced by long-term variations in flame properties along the light probe path. A single scan (10 nm) lasts 8 h, during which it is likely that flame changes in temperature, size, or chemistry, all of which would affect the total absolute losses in the background. This reasoning is supported by the observation that these fluctuations were enhanced in the uncontrolled propane jet, while they remained significantly smaller for the Meker type burner flat flame. For the propane jet, there is little premixing of propane and air, the flame is tall but narrow, and consequently susceptible to air currents or local heating of the gases and the jet nozzle. On the other hand, the Meker type burner has a tightly regulated input gas flow, adequate gas mixing of a fixed ratio of nitrogen and air, and its flame front is short, so that it remains relatively unaffected by air currents. Overall, it remains clear that the increase in baseline noise for the Meker flat flame did not impede observing water vapor transitions with sufficient accuracy to make the derivation of rotational temperatures and water vapor mole fraction possible. In fact, CRDS has proven itself resilient to significant problems caused by harsh, luminous environments.

4. Conclusions

We have demonstrated that it is possible to use CRDS to study ground-state molecular species, in particular water vapor, in hostile environments such as atmospheric flames. From our spectra of overtone transitions of O–H vibrations between 810 nm and 820 nm, we were able to extract rotational temperature and water vapor mole fractions as function of distance from the burner surface, in a straightforward manner.

The study of controlled flames (e.g., a flat flame premixed methane-air burner) proved much easier than study of uncontrolled flames (e.g., propane jet), although spectra were achieved for both. Most importantly, CRDS remained relatively insensitive to the radiative output of the flames and nonuniformities in the flame media did not pose any significant problems to the propagation of ringdown optical signals.

Acknowledgements

This work has been supported by the Office of Basic Energy Research at the Department of Energy (contract: DE-FG03-92ER14303) and DARPA (contract: MDA972-94-1-0003). Jürgen Martin thanks the DAAD for a NATO postdoctoral fellowship.

References

[1] M. Abrams, S. Davis, M. Rao, R. Engleman, J. Brault, Astro. J. Suppl. Ser. 93 (1994) 351.
[2] S. Prucker, W. Meier, W. Stricker, Rev. Sci. Inst. 65 (1994) 2908.
[3] L. Li, X. Xie, M.-C. Lai, Opt. Las. Eng. 24 (1995) 33.
[4] V. Sick, M.N. Bui-Pham, R.L. Farrow, Optics Lett. 20 (1995) 2036.
[5] A. O'Keefe, D.A.G. Deacon, Rev. Sci. Inst. 59 (1988) 2544.
[6] D.D. Romanini, K.K. Lehmann, J. Chem. Phys. 102 (1995) 633.
[7] G. Meijer, M.G.H. Boogaarts, A.M. Wodtke, Chem. Phys. Lett. 217 (1994) 112.
[8] J.T. Hodges, J.P. Looney, R.D. vanZee, Appl. Optics 35 (1996) 4112.
[9] D. Romanini, A.A. Kachanov, N. Sadeghi, F. Stoeckel, Chem. Phys. Lett. 264 (1997) 316.
[10] J. Pearson, A.J. Orr-Ewing, M.N.R. Ashfold, R.N. Dixon, J. Chem. Phys. 106 (1997) 5850.
[11] K. Nakagawa, T. Katsude, A.S. Shelkovnikov, M. de Labachelerie, M. Ohtsu, Optics Comm. 107 (1994) 369.
[12] B.A. Paldus, J. Martin, J. Xie, J.S. Harris, R.N. Zare, J. Appl. Phys., accepted June 1997.
[13] R. Engeln, E. van den Berg, G. Meijer, L. Lin, G.M.H. Knippels, A.F.G. van der Meer, Chem. Phys. Lett. 269 (1997) 293.
[14] J.J. Scherer, D. Voelkel, D.J. Rakestraw, J.B. Paul, C.P. Collier, R.J. Saykally, A. O'Keefe, Chem. Phys. Lett. 245 (1995) 273.
[15] M.G.H. Boogaarts, G. Meijer, J. of Chem. Phys. 102 (1995) 5269.
[16] J.J. Scherer, J.B. Paul, A. O'Keefe, R.J. Saykally, Chem. Rev. 97 (1997) 25.
[17] J.J. Scherer, D.J. Rakestraw, Chem. Phys. Lett. 265 (1997) 169.
[18] M. Kotterer, J.P. Maier, Chem. Phys. Lett. 266 (1997) 342.
[19] P. Zalicki, Y. Ma, R.N. Zare, E.H. Wahl, T.G. Owano, C.H. Kruger, Appl. Phys. Lett. 67 (1995) 144.
[20] R.J. Maniero, Combust. Sci. Technol. 266 (1997) 342.
[21] L.S. Rothman, R.L. Hawkins, R.B. Wattson, R.R. Gamache, J. Quant. Spec. Rad. Trans. 48 (1992) 469.
[22] R.A. Toth, J. Mol. Spec. 166 (1994) 176.
[23] J.M. Flaud, C. Camy-Peyret, A. Bykov, O. Naumenko, T. Petrova, A. Scherbakov, L. Sinitsa, J. Mol. Spec. 183 (1997) 300.
[24] H.W. Kroto, Molecular Rotation Spectra, Dover, New York, 1992.
[25] L. Pierrot, Private Communication 1 (1997) 1.
[26] R.J. Cattolica, Comb. Flam. 44 (1982) 43.
[27] G. Tsatsaronis, Comb. Flam. 33 (1978) 217.